

## Analysis of Unsteady Magnetohydrodynamic Flow of Blood with Slip Conditions in a Permeable Inclined Stretching Vessel

Sham Bansal<sup>1</sup>

<sup>1</sup>Department of Mathematics, Mata Gujri College, Fatehgarh Sahib, Punjab, India

Email ID: [shambansal2010@gmail.com](mailto:shambansal2010@gmail.com)

Cite this paper as: Sham Bansal, (2025) Analysis of Unsteady Magnetohydrodynamic Flow of Blood with Slip Conditions in a Permeable Inclined Stretching Vessel. *Journal of Neonatal Surgery*, 14 (6), 553-564.

### ABSTRACT

This study presents a theoretical examination of time-dependent magnetohydrodynamic flow of blood within a permeable, inclined stretching vessel, incorporating slip conditions to enhance the understanding of blood dynamics in biomedical applications. The porous structure of the vessel naturally impedes the blood's motion. The complex partial differential equations describing this flow were simplified into a set of ordinary differential equations using similarity variables, which were then solved numerically with the Keller-box method. The research systematically analysed how the blood's velocity, temperature, and concentration profiles respond to changes in several key physical parameters. These included the flow's unsteadiness, chemical reaction rates, thermal slip, Prandtl and Schmidt numbers, vessel permeability, velocity slip and magnetic field intensity. Results show these factors significantly alter the fluid's behaviour. A key observation is that higher slip velocity leads to increased temperature and nanoparticle concentration, while simultaneously reducing the fluid's velocity. Furthermore, slip velocity enhances both heat transfer and surface friction. Raising the thermal slip parameter increases the concentration of nanoparticles but lowers the fluid temperature. Additionally, an increase in thermal slip diminishes the rates of heat and mass transport. A higher thermal radiation factor results in an elevated temperature profile.

**Keywords:** Magnetohydrodynamics, Unsteady, Stretching vessel, Porous Medium.

### 1. INTRODUCTION

The intricate dynamics of blood flow within the human circulatory system are fundamental to numerous physiological processes. However, the accurate mathematical modeling of this flow presents a significant challenge due to the complex nature of blood as a fluid and the intricate geometry of the vascular network. Research into unsteady magnetohydrodynamic (MHD) flow of blood within inclined stretching permeable vessels is of particular interest due to its potential applications in targeted drug delivery, medical imaging techniques like MRI, and the treatment of various cardiovascular conditions. Given the inherent complexity of simultaneously considering the unsteady nature of flow, the influence of magnetic fields, the presence of slip at the vessel walls, the stretching of the vessel itself, and the permeability of its boundaries, researchers often rely on a set of simplifying assumptions to make the problem mathematically tractable. The prevalence of investigations in this specific area, as evidenced by the breadth of available literature, highlights its growing importance across various sub-disciplines within biomedical engineering and fluid dynamics.

One of the primary considerations in modeling blood flow is the characterization of blood itself as a fluid. Blood, being an electrolytic solution containing ions and possessing conductive properties due to haemoglobin within red blood cells, exhibits MHD behaviour when exposed to a magnetic field. The primary effect of an applied magnetic field on flowing blood is the generation of a Lorentz force. This force acts perpendicular to both the direction of the blood flow and the direction of the magnetic field, and its effect is to oppose the motion of the fluid, thus providing a mechanism for controlling blood flow. [1] explores the dynamics of blood moving through arteries while subjected to a uniform magnetic field, considering the implications of magneto-hemodynamics. [2] provides an overview of methods for analysing magnetohydrodynamic blood flow. It also compares these methods with those used for non-magnetic blood flow, with a focus on their applications in MRI, drug targeting, and mechanotransduction research. The study in [3] employs numerical techniques to investigate the behaviour of blood flow, modelled as a micropolar fluid, within a channel featuring flexible walls and subjected to an external magnetic field. The analysis specifically examines thermodynamic and magnetohydrodynamic phenomena, taking into account the influence of microrotation, to determine velocity, microrotation, and temperature profiles. A precise mathematical solution for the time-dependent movement of blood, modelled as an electrically conductive, incompressible, and viscoelastic fluid, has been derived by [4]. This solution considers the influence of a magnetic field oriented radially within the pipe.

The porous nature of the vessel wall might lead to different thermal interactions at the boundary compared to a non-permeable wall, potentially making thermal non-equilibrium more significant. Real blood vessel walls, especially capillaries, are permeable, allowing for the exchange of fluids and solutes between the blood and the surrounding tissues. [5] provides an analysis of blood flow under the influence of magnetic fields and fluid dynamics (magnetohydrodynamic flow) within a porous channel. The analysis considers blood as a non-Newtonian fluid, governed by the Walter's B-fluid model. The research presented in [6] explores the intertwined influence of electric and magnetic fields on fluid movement through porous materials. Its main aim is to establish a definition for electro-magneto permeability and to examine how it is affected by various factors. [7] presents an analysis of magnetohydrodynamic blood flow in porous bifurcated arteries, with a focus on heat transfer effects. The study employs a mathematical model solved via the Galerkin least-squares method, which produced stable results for velocity, temperature, pressure, and heat transfer characteristics. Fractional derivatives are utilized in the analysis of Magnetohydrodynamic blood flow through a porous vessel, as presented in [8]. The study [9] uses Adomian's decomposition method to analytically solve for stream function, axial velocity, and wall shear stress in magnetohydrodynamic blood flow through a porous vessel under an external magnetic field, noting significant flow effects.

The geometry and properties of the blood vessel itself also necessitate simplifying assumptions in mathematical models. While real blood vessels exhibit complex and irregular geometries, research often employs idealized shapes such as parallel plates, circular pipes, or cylindrical tubes to represent them. These simplifications allow for the derivation of analytical or semi-analytical solutions. In some cases, the orientation of the vessel is considered, with the assumption that the vessel is inclined at a certain angle to account for the influence of gravity on the blood flow, particularly in larger vessels. [10] analysed magnetohydrodynamic (MHD) blood flow in a porous, inclined artery subjected to an inclined magnetic field. Considering blood as a conductive Newtonian fluid, the research derived formulas for velocity, flow rate, wall shear stress, and pressure. [11] investigated the impact of nanofluids on boundary layer flow across an inclined stretching sheet in porous media, considering a magnetic field. The study in [12] employs the Galerkin method to solve nonlinear partial differential equations and investigate blood flow within an aneurysm under the influence of a static magnetic field. The analysis focuses on characterizing pressure and velocity distributions, as well as wall shear stress, to elucidate how the magnetic field impacts blood flow patterns. A study [13] found that in an inclined cylindrical tube with a magnetic field, the field slows blood flow (Lorentz effect), while increased inclination speeds it up. [14] presents analytical solutions for magnetohydrodynamic bio-fluid flow in branched arteries with an angled magnetic force, revealing two solutions for axial velocity and temperature based on magnetic drag and porosity.

The interaction between the blood and the vessel wall is often modeled using slip conditions, where the fluid velocity at the wall is not necessarily zero, in contrast to the conventional no-slip condition which assumes zero relative velocity between the fluid and the solid boundary. The consideration of slip conditions becomes particularly relevant for blood flow in micro-vessels with permeable walls, as the fluid exchange and the porous nature of the wall can lead to a non-zero fluid velocity at the boundary. In the context of blood flow, while typically less significant at macroscopic scales, thermal slip also play a role in specific scenarios such as within the narrow confines of capillaries or under conditions of rapid heat transfer at the vessel wall, as could be encountered in certain therapeutic applications. For instance, Snippet suggests that enhancing thermal slip could be advantageous for achieving faster cooling of capillary surfaces during medical treatments. [15] investigated unsteady blood flow in a narrowed artery, incorporating velocity slip and using a Bingham plastic model. It found that velocity, shear stress, and flow rate decreased over time and along the artery's length. [16] analytically investigates unsteady non-Newtonian blood flow in a stenosed artery with slip, focusing on how slip velocity, body acceleration, and magnetic fields affect axial velocity, wall shear stress, and flow rate. [17] studies the role of Thermal Wall and Velocity Slips in Non-Darcy MHD boundary layer nanofluid flow along a non-linear stretching sheet. Study [18] found that increased slip accelerates unsteady capillary flow (imbibition), but its analysis of slip in laminar flows didn't specifically cover unsteady blood flow under slip conditions.

Finally, the unsteady nature of blood flow, driven by the pulsatile pumping action of the heart, is a critical aspect to consider. This unsteadiness is typically incorporated into mathematical models by including time-dependent terms in the governing equations and boundary conditions. The unsteady flow or boundary conditions might be modeled using specific mathematical functions, such as sinusoidal functions to represent the periodic nature of pulsatile flow, or functions describing the temporal evolution of stretching velocity or surface temperature. [19] examines heat transfer effects on unsteady MHD blood flow within a permeable vessel. [20] computationally and mathematically simulated 2D unsteady laminar flow in a bifurcated artery with an aneurysm. [21] theoretically investigated the treatment and slip effects on MHD blood flow through a stenotic artery with a porous wall and boundary slip. [22] examined thermal radiation's impact on unsteady MHD blood flow in a stretching permeable capillary. The unsteady magnetohydrodynamic blood flow of a visco-elastic fluid in an inclined, porous, and stenosed artery, considering body acceleration and slip, was analysed by [23]. [24] explored the combined effects of thermal energy and material transport on the flow characteristics of blood, specifically considering its behaviour as a Casson fluid under the influence of a magnetic field within a vessel undergoing stretching and exhibiting permeability.

While numerous studies have investigated MHD blood flow under various conditions, a significant area requiring further exploration involves the combined complexities presented by unsteady flow dynamics within a permeable, inclined, and

stretching vessel, particularly when realistic slip boundary conditions and chemical reactions are simultaneously considered. Addressing this identified research gap holds considerable potential for significantly advancing our understanding of blood flow in a range of complex physiological and pathological conditions. The study of blood flow in permeable vessels has focused on understanding the exchange of substances across the vessel wall, which is crucial for nutrient and waste transport. These factors are critical as they significantly impact the blood flow dynamics and heat transmission characteristics, presenting opportunities to enhance efficiency in various engineering applications. The outcomes anticipated from this research endeavour are expected to facilitate the development of advanced technologies across a multitude of scientific and engineering disciplines.

## 2. MATHEMATICAL FORMULATION

This investigation aims to elucidate the complex interplay of thermal slip, velocity slip, and magnetohydrodynamic forces in shaping the structural attributes of both the hydrodynamic and thermal boundary layers within the specified blood flow regime. The study undertakes a comprehensive analysis of the unsteady magnetohydrodynamic flow of blood, subject to slip boundary conditions, within a vessel characterized by inclination, extensibility and permeability. The study specifically focuses on a two-dimensional, unsteady, laminar, and incompressible flow regime for the blood. The model incorporates slip boundary conditions at the interface between the blood and the vessel wall, allowing for a non-zero tangential velocity of the fluid at the solid boundary. The study accounts for an externally applied magnetic field with spatially varying intensity to investigate its heterogeneous influence on the dynamics of blood flow within the vessel. The blood vessel is assumed to maintain a spatially uniform temperature ( $T_w$ ) along its entire length. The temperature ( $T_\infty$ ) of the blood at a sufficiently distance from the stretching vessel is assumed to remain uniform. The concentration ( $C_w$ ) of blood constituents is assumed to be spatially homogeneous within the vessel, and a uniform concentration ( $C_\infty$ ) is also maintained in the bulk fluid region distant from the vessel. The physical configuration for this research is shown in Figure 1. [22] previously laid out the mathematical formulation and boundary constraints relevant to this problem. The blood flow analysis presented next relies on the following four related equations:

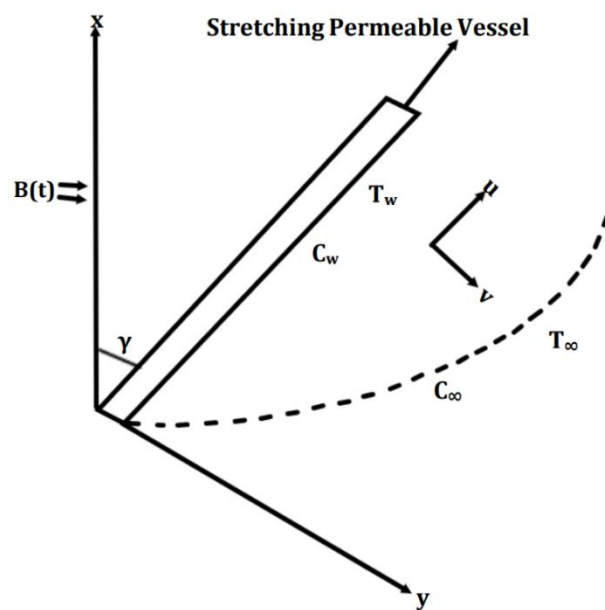


Figure 1 Physical Setup for the current research problem

$$\frac{\partial u}{\partial x} + \frac{\partial v}{\partial y} = 0 \quad (1)$$

$$\frac{\partial u}{\partial t} + u \frac{\partial u}{\partial x} + v \frac{\partial u}{\partial y} = \frac{\mu}{\rho} \frac{\partial^2 u}{\partial y^2} + [g\beta_T(T - T_\infty) + g\beta_C(C - C_\infty)]\cos(\gamma) - \frac{\sigma(B(t))^2}{\rho} u - \frac{\mu}{\rho} \frac{1}{K_d(t)} u \quad (2)$$

$$\frac{\partial T}{\partial t} + u \frac{\partial T}{\partial x} + v \frac{\partial T}{\partial y} = \frac{\mu}{\rho c_p} \left( \frac{\partial u}{\partial y} \right)^2 + \alpha \frac{\partial^2 T}{\partial y^2} + \frac{1}{\rho c_p} \frac{\partial q_r}{\partial y} \quad (3)$$

$$\frac{\partial C}{\partial t} + u \frac{\partial C}{\partial x} + v \frac{\partial C}{\partial y} = D_m \frac{\partial^2 C}{\partial y^2} - Kr(t)(C - C_\infty) \quad (4)$$

Considering a variable magnetic field defined by  $B(t) = \frac{B_0}{\sqrt{1-ct}}$ ,  $B_0$  denotes the magnetic field strength at  $t = 0$ ,  $K_d(t) =$

$K_0(1 - ct)$  portrays the time dependent permeability parameter, where  $c \geq 0$  is a real number such that  $ct < 1$ . Thermal diffusivity  $\alpha = \frac{\kappa}{\rho c_p}$  and effective heat capacity ratio  $\tau = \frac{(\rho c_p)_s}{(\rho c_p)_f}$ .  $Kr(t) = \frac{Kr}{1 - ct}$  is the chemical rate of the blood flow.  $\beta_c$  and  $\beta_T$  are concentration and thermal expansion coefficients respectively and  $\gamma$  is inclination angle.

$$C = C_w, u = u_w + N v_f \frac{\partial u}{\partial y} = \frac{ax}{1 - ct} + N_0 \frac{\sqrt{1 - ct}}{x} \cdot v_f \frac{\partial u}{\partial y},$$

$$v = v_w = -\sqrt{\frac{v_f u_w}{x}} S \text{ \& } T = T_w + D \frac{\partial T}{\partial y} = T_\infty + \frac{ax}{1 - ct} + D_0 \frac{\sqrt{1 - ct}}{x} \text{ at } y = 0$$

and  $u \rightarrow 0, v \rightarrow 0, T \rightarrow T_\infty, C \rightarrow C_\infty$  if  $y \rightarrow \infty$  (5)

Equation (5) specifies the boundary conditions that dictate the behaviour of the velocity and thermal slips in the vicinity of the stretching surface. Specifically, the velocity slip, denoted by the symbol  $N$ , is mathematically defined as  $N_0 \sqrt{1 - ct}$ , while the thermal slip,  $D$ , is mathematically defined as  $D_0 \sqrt{1 - ct}$ . Here,  $N_0$  and  $D_0$  represent the initial magnitudes of the velocity and thermal slips, respectively. Furthermore, the temperature of the sheet  $T_w$  is determined by  $T_\infty + \frac{ax}{1 - ct}$  and the stretching velocity  $u_w$  is defined by  $\frac{ax}{1 - ct}$ , where 'a' indicates the rate of stretching. Applying the Rosseland approximation, the radiative heat flux can be formulated as  $q_r = -\frac{4\sigma^* \partial T^4}{3k^* \partial y}$ , the parameters  $\sigma^*$  and  $k^*$  symbolize the Stefan-Boltzmann constant and the Rosseland mean absorption coefficient, respectively. Given that the temperature variations within the blood mass inside the capillary are minimal, employing Taylor series expansion, we can approximate, we write:  $T^4 = T_\infty^4 + 4T_\infty^3(T - T_\infty) + 6T_\infty^2(T - T_\infty)^2 + \dots \cong 4T_\infty^3T - 3T_\infty^4$ , when higher-order terms are disregarded.

Similarity transformations can be described as:

$$\theta(\eta) = \frac{T - T_\infty}{T_w - T_\infty}, v = -\left(\frac{a v_f}{(1 - ct)}\right)^{\frac{1}{2}} f(\eta), \eta = y \left(\frac{a}{(1 - ct)v_f}\right)^{\frac{1}{2}}, u = \frac{ax}{1 - ct} f'(\eta) \text{ and } \xi(\eta) = \frac{C - C_\infty}{C_w - C_\infty} \quad (6)$$

Introduce the stream function,  $\psi(x, y)$ , which satisfies equation (1), stated as:

$$u = \frac{\partial \psi}{\partial y} \text{ \& } v = -\frac{\partial \psi}{\partial x} \quad (7)$$

Applying the transformations defined by equations (6–7) to equations (2–4) results in the subsequent set of non-dimensional ODEs:

$$f''''(\eta) + f''(\eta)f(\eta) - [Gr_x\theta(\eta) + Gc_x\xi(\eta)]\cos(\gamma) - P\left(f'(\eta) + \frac{\eta}{2}f''(\eta)\right) - (f'(\eta))^2 - f'(\eta)\left(M^2 + \frac{1}{K}\right) = 0 \quad (8)$$

$$(1 + Q)\theta''(\eta) + Pr\left[f(\eta)\theta'(\eta) - \theta(\eta)f'(\eta) - P\left(\theta(\eta) + \frac{\eta}{2}\theta'(\eta)\right) + Ec(f''(\eta))^2\right] = 0 \quad (9)$$

$$\xi''(\eta) + Sc\left[\xi'(\eta)f(\eta) - \xi(\eta)f'(\eta) - P\left(\xi(\eta) + \frac{\eta}{2}\xi'(\eta)\right)\right] - Kr\xi(\eta) = 0 \quad (10)$$

The boundary restrictions outlined in equation (5) are transformed using the relationship defined by equation (6) into:

$$\theta(\eta) = 1 + \beta\theta'(0), f(\eta) = S, \xi(\eta) = 1 \text{ and } f'(\eta) = 1 + \lambda f''(0) \text{ for } \eta = 0$$

$$\text{and } \xi(\eta) \rightarrow 0, f'(\eta) \rightarrow 0, \theta(\eta) \rightarrow 0 \text{ when } \eta \rightarrow \infty \quad (11)$$

The parameters are set up in the following way:

$$P = \frac{c}{(1 - ct)v_f}, Gc_x = \frac{g\beta_c(C_w - C_\infty)(1 - ct)^2}{a^2x}, \beta = D_0 \left(\frac{a}{v_f}\right)^{\frac{1}{2}}, K = \frac{K_0(1 - ct)}{v_f}$$

$$Ec = \frac{x^2 a^2}{(1 - ct)^2(T_w - T_\infty)c_p}, Pr = \frac{v_f}{\alpha}, \lambda = N_0 (av_f)^{\frac{1}{2}}, Q = \frac{16\sigma^* T_\infty^3}{3k^* k}$$

$$M = \left(\frac{\sigma}{\rho a}\right)^{\frac{1}{2}} B_0, Gr_x = \frac{g\beta_T(T_w - T_\infty)(1 - ct)^2}{a^2x}, Sc = \frac{v_f}{D_m} \quad (12)$$

This study primarily examines the mass transfer rate ( $-\xi'(0)$ ), skin friction coefficient ( $f''(0)$ ) and heat transmission rate ( $-\theta'(0)$ ). Their mathematical expressions are given by:

$$-\xi'(0) = Sh(Re_x)^{1/2}, f''(0) = C_f(Re_x)^{1/2}$$

$$\text{and } -\theta'(0) = \frac{Nu}{1+Q} (Re_x)^{-1/2} \quad (13)$$

Sherwood number  $Sh$  is a dimensionless quantity used to measure the effectiveness of convective mass transfer. The local Reynolds number  $Re_x$  is another dimensionless parameter that describes the nature of the fluid flow. Skin friction  $C_f$  represents the shear stress at the surface, while the Nusselt number  $Nu$  is a dimensionless ratio that indicates the rate of convective heat transfer.

### 2.1 Adopted Computational Method

The system of non-dimensional ODEs, represented by Equations (8–10), associated to boundary restrictions (11), were computed through FDKBI technique. Within the context of this study, the FDKBI approach is a robust numerical technique for computing boundary value problems, particularly those arising from systems of coupled, non-linear ODEs. Its inherent stability and accuracy make it an ideal choice for this investigation. Originally devised by [25], the FDKBI is known for its stability, efficiency, and relatively straightforward implementation, making it a popular choice for tackling fluid flow and heat transmission problems. The FDKBI method comprises four main stages:

1. **Decomposition:** A set of  $n$ th-order nonlinear ODEs are transformed into  $n$  first-order nonlinear ODEs.
2. **Discretization:** Subsequently, the resulting system is then discretized using finite difference approximations, yielding a set of nonlinear algebraic equations.
3. **Linearization:** Linearizing these algebraic equations using Newton's method.
4. **Solving the System:** Solving the linearized system of equations iteratively using a specialized elimination technique that exploits the block-tridiagonal structure.

### 3. RESULTS AND DISCUSSION

This research delves into the time-dependent MHD flow of blood within an angled porous stretching vessel, incorporating the influences of velocity and thermal slip at the boundary. By scrutinizing the intricate interactions among various parameters, including the unsteady factor ( $P$ ), magnetic factor ( $M$ ), suction actor ( $S$ ), thermal slip ( $\beta$ ), Eckert number ( $Ec$ ), chemical reaction factor ( $Kr$ ), Prandtl number ( $Pr$ ), Grashof number  $Gr_x$ , modified Grashof number  $Gc_x$ , permeability factor ( $K$ ), Schmidt number ( $Sc$ ), inclination angle ( $\gamma$ ), radiation factor ( $Q$ ) and velocity slip ( $\lambda$ ) on the velocity ( $f'(\eta)$ ), concentration ( $\xi(\eta)$ ) and temperature ( $\theta(\eta)$ ) and the characteristics of the boundary layer, thereby contributing significantly to the understanding of complex fluid dynamics. Grasping these effects is crucial for forecasting and regulating fluid behavior across numerous medical applications. The governing equations are solved numerically utilizing the FDKBI method, with the resultant solutions presented in graphical form. For the numerical analysis, the following standard values for the physical parameters were utilized:  $Gr_x = Gc_x = 2$ ,  $M^2 = S = Sc = 0.5$ ,  $P = 0.3$ ,  $Pr = 6.8$ ,  $Kr = K = Q = \lambda = Ec = \beta = 0.2$  and  $\gamma = 60^\circ$ , unless otherwise indicated.

The analysis reveals that velocity and thermal slips exert a significant influence in the temperature profile and flow trends. Figures (2–3) demonstrate that increasing the thermal slip factor  $\beta$  leads to a hike in concentration while simultaneously decreasing the blood temperature.

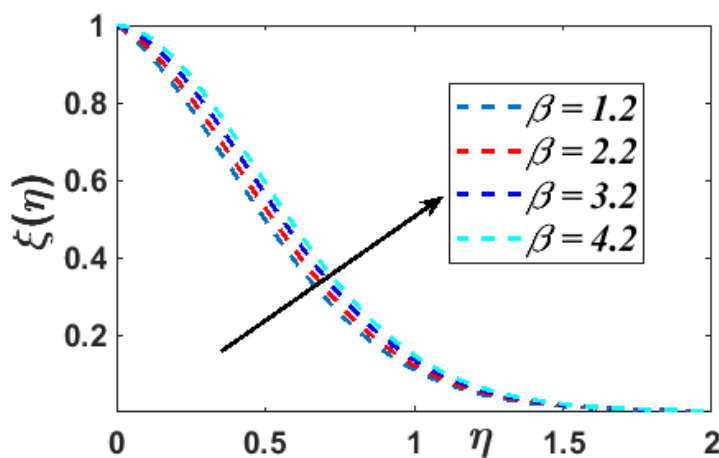


Figure 2 Impact of thermal slip factor  $\beta$  on Concentration

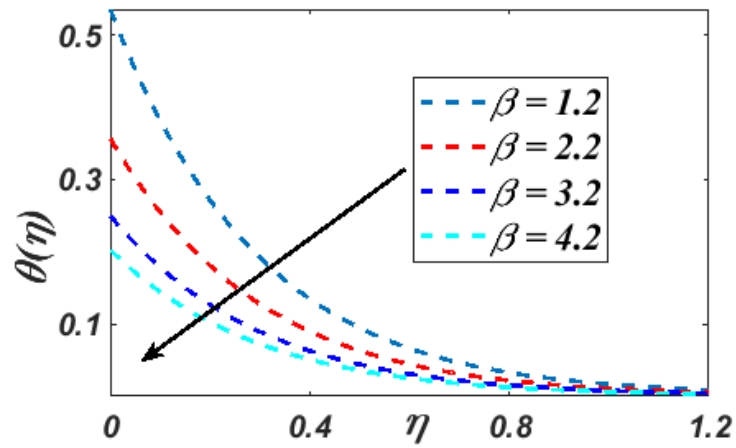


Figure 3 Impact of thermal slip factor  $\beta$  on Temperature

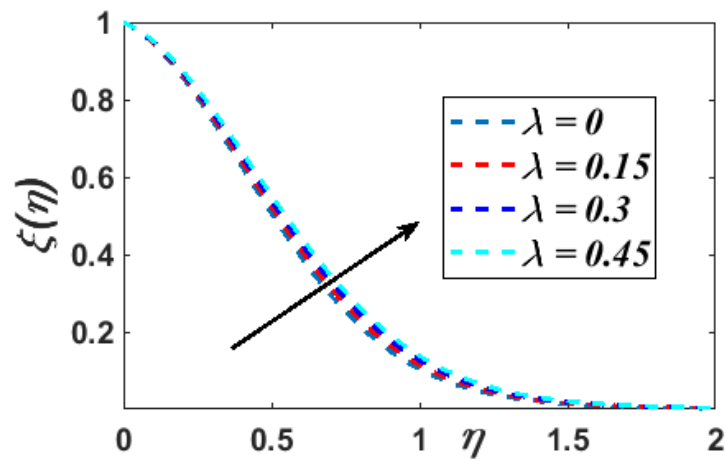


Figure 4 Impact of velocity slip factor  $\lambda$  on Concentration

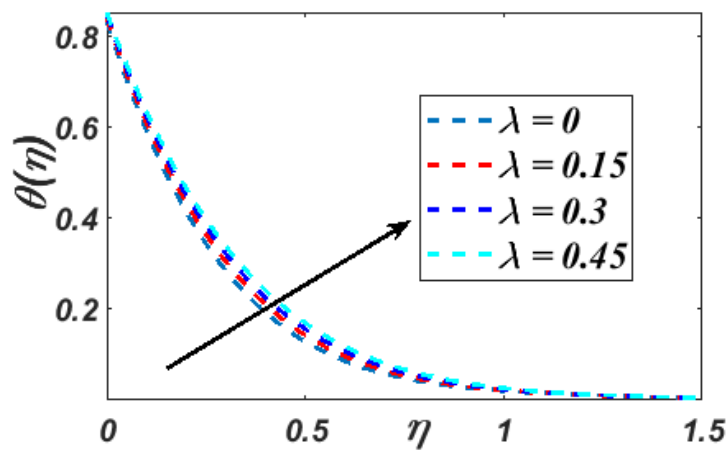
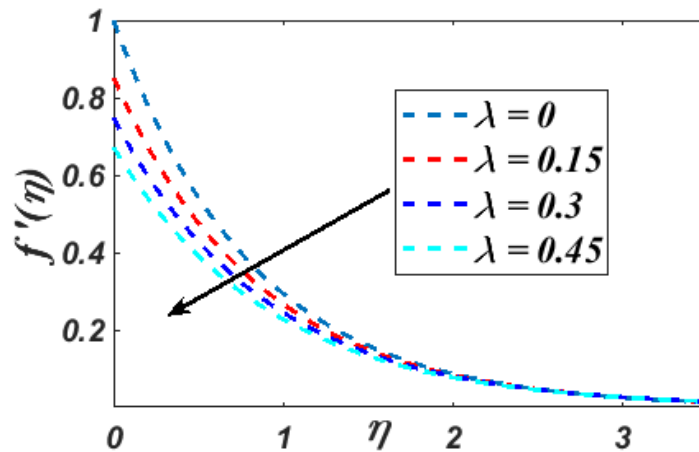
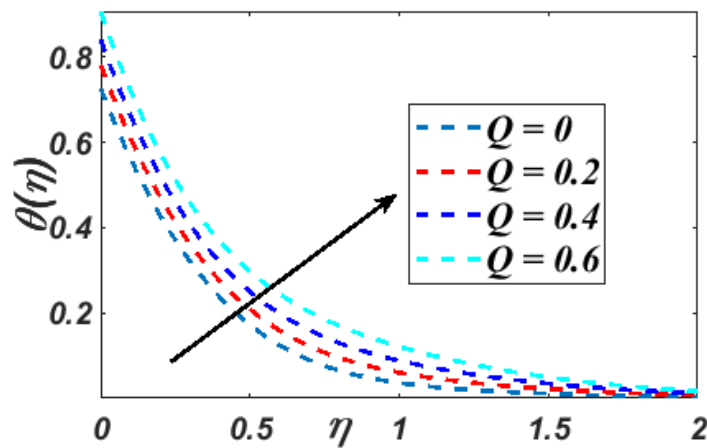


Figure 5 Impact of velocity slip factor  $\lambda$  on Temperature



Figure 6 Impact of velocity slip factor  $\lambda$  on VelocityFigure 7 Impact of thermal radiation factor  $Q$  on Temperature

A rise in the velocity slip parameter  $\lambda$  results in an enhancement of both temperature  $\theta(\eta)$  and concentration  $\xi(\eta)$ , while the velocity profile  $f'(\eta)$ , as demonstrated in Figures (4-6), exhibits the opposite behaviour, decreasing with increasing  $\lambda$ . The occurrence of both velocity and thermal slip factors causes significant changes in the temperature and concentration profiles within the blood flow. Furthermore, the temperature profiles increase with a rise in the thermal radiation factor  $Q$ , which is visually illustrated by Figure 7.

**Table 1** Computational results for  $-f''(0)$ ,  $-\xi'(0)$  and  $-\theta'(0)$  across numerous values of  $\lambda$ ,  $\gamma$  and  $\beta$ , when  $M^2 = S = Sc = P = Q = 0.5$ ,  $Pr = 22$ ,  $Kr = K = Ec = 0.4$ ,  $Gr_x = Gc_x = 2$ .

$\gamma$	$\beta$	$-\xi'(0)$		$-f''(0)$		$-\theta'(0)$	
		$\lambda = 0.5$	$\lambda = 1$	$\lambda = 0.5$	$\lambda = 1$	$\lambda = 0.5$	$\lambda = 1$
$30^\circ$	0.5	0.702547	0.743607	0.448816	0.407644	0.850672	0.842237
$45^\circ$	0.5	0.697540	0.738308	0.502545	0.456444	0.847809	0.839422
$60^\circ$	0.5	0.692569	0.733046	0.562706	0.511086	0.844956	0.836597
$30^\circ$	1	0.493431	0.522270	0.448816	0.407644	0.651706	0.645244
$45^\circ$	1	0.489914	0.518267	0.502545	0.456444	0.649513	0.643072
$60^\circ$	1	0.486422	0.514573	0.562706	0.511086	0.647327	0.640908

The numerical outcomes presented in Table 1 elucidate the computational findings for  $-f''(0)$ ,  $-\xi'(0)$  and  $-\theta'(0)$  across various values of  $\lambda$ ,  $\gamma$  and  $\beta$ . These calculations were conducted under uniform parameter settings for factors  $M^2 = S =$

$Sc = P = Q = 0.5$ ,  $Pr = 22$ ,  $Kr = K = Ec = 0.4$ ,  $Gr_x = Gc_x = 2$ . A noteworthy discovery is that an increase in the thermal slip factor  $\beta$ , results in a reduction of heat and mass transport. This diminishing trend is associated with decreased surface friction. The skin friction coefficient exhibits insensitivity to variations in  $\beta$ . Furthermore, an elevation in the inclination angle  $\gamma$  results in decreased efficiency of both mass and heat transfer while concurrently increasing the drag on the surface, as evidenced by the skin friction coefficient. This finding underscores the capacity of  $\gamma$  to hinder fluid dynamics and influence transport phenomena. Additionally, an augmented slip velocity  $\lambda$  adjacent to the wall enhances thermal transmission and surface friction. Nonetheless, this improvement is accompanied by a reduction in mass transfer rates.

### 3.1 Code Validation

The reliability of the present findings was confirmed by benchmarking against the published results of Misra et al. [22]. While acknowledging the limitations inherent in their models (specifically,  $\gamma = 90^\circ$  and  $Sc = Kr = 0$ ). Table 2 presents a quantitative comparison of  $-\theta'(0)$  across various values of  $P$ ,  $M^2$  and  $Pr$ , demonstrating agreement with our data.

**Table 2** Comparative analysis for  $-\theta'(0)$  across numerous values of  $P$ ,  $M^2$  and  $Pr$ , when  $S = 0.5$ ,  $Sc = 0$ ,  $Kr = Gr_x = Gc_x = 0$ ,  $K = 0.4$ ,  $Q = 1$ ,  $\lambda = 2.5$ ,  $\beta = 1$  and  $\gamma = 90^\circ$ .

$P$	$M^2$	$Pr$	$-\theta'(0)$	
			Misra et al. [22]	Present Results
3	0.5	21	0.465913	0.465914
3	0.5	25	0.533551	0.533552
3	1	21	0.424202	0.424204
4	0.5	21	0.390481	0.390482

## 4. CONCLUSIONS

The focus of this research is the modelling of time-varying MHD blood flow within an angled, porous, and stretching vascular structure. Boundary conditions incorporating both velocity and thermal slip are explicitly included in the model. The FDKBI technique was employed to compute numerical results. This work underscores the complex interactions among the governing factors and their significance in predicting flow behaviour. Through comprehensive analysis, the distinct and combined effects of these parameters on the temperature, concentration, and velocity profiles are elucidated. Notable outcomes of this research encompass:

1. Slip velocity  $\lambda$  augments temperature and concentration, but velocity exhibits an inverse trend. Moreover,  $\lambda$  improves heat transmission and surface friction.
2. Increasing the thermal slip  $\beta$  enhances nanoparticle concentration while lowering fluid temperature. Also, an increase in the thermal slip factor  $\beta$ , results in a reduction of heat and mass transport. The skin friction coefficient exhibits insensitivity to variations in  $\beta$ .
3. A hike in the thermal radiation factor causes an enhancement in temperature profile.
4. An elevation in the inclination angle  $\gamma$  results in decreased efficiency of both mass and heat transfer while concurrently increasing the drag on the surface

ABBREVIATIONS	
$B_0$	Uniform magnetic field strength
$B(t)$	Variable magnetic field strength
$P$	Unsteady Factor
$a$	Stretching rate
$C$	Concentration of blood



$Pr$	Prandtl number
$C_f$	Skin-friction
$Q$	Thermal radiation parameter
$C_p$	specific heat
$C_\infty$	Concentration of the free stream
$S$	Suction/injection parameter
$C_w$	Concentration of the stretching vessel
$Kr$	Chemical reaction factor
$Sc$	Schmidt number
$D_m$	Brownian diffusion Coefficient
$f(\eta)$	Dimensionless stream function
$Ec$	Eckert number
$-f''(0)$	Skin friction coefficient
$D_0$	Initial thermal slip
$g$	Acceleration due to gravity
$f'(\eta)$	Non dimensional velocity
$M$	Magnetic parameter
$Gr_x$	Local Grashof number
$N_0$	Initial velocity slip
$Gc_x$	Local modified Grashof number
$Pr$	Prandtl number
$K_d$	Dimensional permeability parameter
$K$	Non-dimensional permeability parameter
$Nu$	Nusselt number
$Sh$	Sherwood number
$u$	Velocity component parallel to the $x$ direction
$T$	Dimensional temperature of the blood
$Re$	Reynolds number
$T_\infty$	Free stream temperature
$x, y$	Cartesian coordinate axis
$T_w$	Vessel temperature
$v$	Velocity component parallel to the $y$ direction
$D$	Thermal slip factor
$u_w$	Stretching velocity
<b>Greek Letters</b>	

$\eta$	Non-dimensional similarity variable
$\beta$	Non-dimensional thermal slip factor
$\kappa$	Thermal conductivity
$\beta_T$	Thermal expansion coefficient
$\lambda$	Non-dimensional velocity slip factor
$\beta_c$	Concentration expansion coefficient
$\gamma$	Inclination parameter
$\xi(\eta)$	Non-dimensional concentration
$\kappa_f$	Thermal conductivity of blood
$\theta(\eta)$	Non-dimensional temperature
$\sigma$	Electric conductivity
$\phi$	Nanoparticles solid volume fraction
$\alpha_f$	Blood thermal diffusivity
$\tau_w$	Wall shear stress
$\nu_f$	Blood kinematic viscosity
$\mu_f$	Blood viscosity
$\rho_f$	Blood density
$\rho C_p$	Heat capacitance of blood
$-\theta'(0)$	Local Nusselt number
$\psi$	Stream function
$-\xi'(0)$	Local Sherwood number

**Conflict of Interest:** The authors declare no conflicts of interest.

**Data Availability:** Data will be made available on reasonable request.

## REFERENCES

- [1] Haider, J. A., Ahmad, S., Ghazwani, H. A., Hussien, M., Almusawa, M. Y., & Az-Zo'bi, E. A. (2024). *Results validation by using finite volume method for the blood flow with magnetohydrodynamics and hybrid nanofluids. Modern Physics Letters B*, 38(24). <https://doi.org/10.1142/s0217984924502087>
- [2] Drochon, A., Beuque, M., & Abi-Abdallah Rodriguez, D. (2018). A Review of Some Reference Analytic Solutions for the Magnetohydrodynamic Flow of Blood. *Applied Mathematics-a Journal of Chinese Universities Series B*, 09(10), 1179–1192. <https://doi.org/10.4236/AM.2018.910078>
- [3] Misra, J. C., Chandra, S., Shit, G. C., & Kundu, P. K. (2013). Thermodynamic and magnetohydrodynamic analysis of blood flow considering rotation of micro-particles of blood. *Journal of Mechanics in Medicine and Biology*, 13(01), 1350013. <https://doi.org/10.1142/S0219519413500139>
- [4] Elshehawey, E. F., Elbarbary, E. M. E., Afifi, N. A. S., & El-Shahed, M. (2000). MHD flow of an elastico-viscous fluid under periodic body acceleration. *International Journal of Mathematics and Mathematical Sciences*, 23(11), 795–799. <https://doi.org/10.1155/S0161171200002817>
- [5] Misra, J. C., Sinha, A., & Shit, G. C. (2011). A numerical model for the magnetohydrodynamic flow of blood in a porous channel. *Journal of Mechanics in Medicine and Biology*, 11(03), 547–562. <https://doi.org/10.1142/S0219519410003794>

- [6] Majumdar, P., & Dasgupta, D. (2023). Electromagnetohydrodynamic (EMHD) flow through porous media—Multiscale approach. *Journal of Applied Physics*, 134 (22). <https://doi.org/10.1063/5.0174534>
- [7] Zain, N., & Ismail, Z. (2023). Dynamic Response of Heat Transfer in Magnetohydrodynamic Blood Flow Through a Porous Bifurcated Artery with Overlapping Stenosis. *Journal of Advanced Research in Fluid Mechanics and Thermal Sciences*, 101(1), 215–235. <https://doi.org/10.37934/arfmts.101.1.215235>
- [8] Ayaz, F., & Heredağ, K. (2024). Fractional model for blood flow under MHD influence in porous and non-porous media. *An International Journal of Optimization and Control Theories & Applications (IJOCTA)*, 14(2), 156–167. <https://doi.org/10.11121/ijocta.1497>
- [9] Sinha, A., & Shit, G. C. (2015). Modeling of Blood Flow in a Constricted Porous Vessel Under Magnetic Environment: An Analytical Approach. *International Journal of Applied and Computational Mathematics*, 1(2), 219–234. <https://doi.org/10.1007/S40819-014-0022-6>
- [10] Srivastava, N. (2014). Analysis of Flow Characteristics of the Blood Flowing through an Inclined Tapered Porous Artery with Mild Stenosis under the Influence of an Inclined Magnetic Field. *Journal of Biophysics*, 2014, 797142. <https://doi.org/10.1155/2014/797142>
- [11] Bansal, S., Pal, J., Bisht, M. S., & Fartyal, P. (2024). Influence of Nanofluids on Boundary Layer Flow over an Inclined Stretching Sheet in a Porous Media along with Magnetic Field. *International Journal of Mathematical, Engineering and Management Science*, 9(2), 267–282. <https://doi.org/10.33889/IJMEMS.2024.9.2.014>
- [12] Raptis, A., Xenos, M., Tzirtzilakis, E. E., & Matsagkas, M. (2014). Finite element analysis of magnetohydrodynamic effects on blood flow in an aneurysmal geometry. *Physics of Fluids*, 26(10), 101901. <https://doi.org/10.1063/1.4895893>
- [13] Hussain, L., Uddin, S., & Syed Asif, S. A. (2023). Unsteady and Incompressible Magneto-Hydrodynamics Blood Flow in an Inclined Cylindrical Channel. *International Journal of Physics Research and Applications*, 6(2), 154–159. <https://doi.org/10.29328/journal.ijpra.1001065>
- [14] Ahmed, K. K., Ahmed, S., & Chamkha, A. (2023). Impact of Inclined Magnetic Force on Bio-Fluid in Permeable Bifurcated Arteries: Analytical Approach. *Journal of Nanofluids*, 12(2), 332–340. <https://doi.org/10.1166/jon.2023.2000>
- [15] Geeta, & Siddiqui, S. U. (2016). Analysis of Unsteady Blood Flow through Stenosed Artery with Slip Effects. *International Journal of Bio-Science and Bio-Technology*, 8(5), 43–54. <https://doi.org/10.14257/ijbsbt.2016.8.5.0>
- [16] Nandal, J., Kumari, S., & Rathee, R. (2019). The Effect of Slip Velocity on Unsteady Peristalsis MHD Blood Flow through a Constricted Artery Experiencing Body Acceleration. *International Journal of Applied Mechanics and Engineering*, 24(3), 645–659. <https://doi.org/10.2478/IJAME-2019-0040>
- [17] Bansal, S., Kumar, A., Pal, J., Goyal, I., & Negi, A. S. (2024). Influence of Thermal Wall and Velocity Slips on Non-Darcy MHD Boundary Layer Flow of a Nanofluid over a Non-linear Stretching Sheet. *Journal of Physics: Conference Series*, 2844, 012018. <https://doi.org/10.1088/1742-6596/2844/1/012018>
- [18] Yap, E. J., Eny, G. E., Hona, J., & Azese, M. N. (2025). Generalized Navier-slip approach for steady flows in common ducts and unsteady capillary slip-flow. *Physics of Fluids*, 37(1). <https://doi.org/10.1063/5.0248768>
- [19] Sinha, A., Misra, J., & Shit, G. (2016). Effect of heat transfer on unsteady MHD flow of blood in a permeable vessel in the presence of non-uniform heat source. *Alexandria Engineering Journal*, 55(3), 2023–2033. <https://doi.org/10.1016/j.aej.2016.07.010>
- [20] Hussain, A., & Tag-Eldin, E. (2023). Mathematical analysis of unsteady blood flow through bifurcated abdominal aorta featured aneurysm. *Alexandria Engineering Journal*, 75, 589–604. <https://doi.org/10.1016/j.aej.2023.06.022>
- [21] Omamoke, E., & Amos, E. (2023). Treatment and Slip Effect on MHD Blood Flow through a Stenotic Artery: A Mathematical Model. *Asian Research Journal of Mathematics*, 19(6), 61–76. <https://doi.org/10.9734/arjom/2023/v19i6666>
- [22] Misra, J. C., & Sinha, A. (2013). Effect of thermal radiation on MHD flow of blood and heat transfer in a permeable capillary in stretching motion. *Heat and Mass Transfer*, 49(5), 617–628. <https://doi.org/10.1007/s00231-012-1107-6>
- [23] Manisha, R., & Kumar, S. (2022). Visco-Elastic Fluid Model in an Inclined Porous Stenosed Artery with Slip Effect and Body Acceleration. *International Journal of Applied Mechanics and Engineering*, 27(4), 82–104. <https://doi.org/10.2478/ijame-2022-0052>
- [24] Sitamahalakshmi, V., Reddy, G. V. R., & Falodun, B. O. (2023). Heat and mass transfer effects on MHD casson

fluid flow of blood in stretching permeable vessel. *Journal of Applied Nonlinear Dynamics*, 12(1), 87–97. <https://doi.org/10.5890/jand.2023.03.006>

- [25] Keller, H. B., & Cebeci, T. (1972). Accurate numerical methods for boundary-layer flows. ii: Two dimensional turbulent flows. *AIAA Journal*, 10(9), 1193–1199. <https://doi.org/10.2514/3.50349>
-